

# PIPsUS: Self-Supervised Dense Point Tracking in Ultrasound\*

Wanwen Chen<sup>1</sup>, Adam Schmidt<sup>1</sup>, Eitan Prisman<sup>2</sup>, and Tim Salcudean<sup>1,3</sup>

<sup>1</sup> Department of Electrical and Computer Engineering, The University of British Columbia, Vancouver, BC, Canada

<sup>2</sup> Division of Otolaryngology, Department of Surgery, Vancouver General Hospital, Vancouver, BC, Canada

<sup>3</sup> School of Biomedical Engineering, The University of British Columbia, Vancouver, BC, Canada  
{wanwenc,tims}@ece.ubc.ca

**Abstract.** Finding point-level correspondences is a fundamental problem in ultrasound (US), since it can enable US landmark tracking for intraoperative image guidance in different surgeries, including head and neck. Most existing US tracking methods, e.g., those based on optical flow or feature matching, were initially designed for RGB images before being applied to US. Therefore domain shift can impact their performance. Training could be supervised by ground-truth correspondences, but these are expensive to acquire in US. To solve these problems, we propose a self-supervised pixel-level tracking model called PIPsUS. Our model can track an arbitrary number of points in one forward pass and exploits temporal information by considering multiple, instead of just consecutive, frames. We developed a new self-supervised training strategy that utilizes a long-term point-tracking model trained for RGB images as a teacher to guide the model to learn realistic motions and use data augmentation to enforce tracking from US appearance. We evaluate our method on neck and oral US and echocardiography, showing higher point tracking accuracy when compared with fast normalized cross-correlation and tuned optical flow. Code will be available once the paper is accepted.

**Keywords:** Dense point tracking · Ultrasound · Self-supervised learning · Landmark tracking.

## 1 Introduction

Intraoperative ultrasound (US) in head and neck surgery is an emerging tool helping surgeons localize tumors and important anatomy such as arteries. Key-point tracking can assist surgeons in finding and keeping tissue of interest in the

---

\* Supported by NSERC Discovery Grant and Charles Laszlo Chair in Biomedical Engineering held by Dr. Salcudean, VCHRI Innovation and Translational Research Awards, and the University of British Columbia Department of Surgery Seed Grant held by Dr. Prisman.

US plane, as well as estimating relative transducer motion [24]. Moreover, finding point-level correspondences in US can benefit many clinical applications, such as large strain estimation and image registration, where deformation can be modeled by the motion of control points. Sparse feature matching and optical flow are two different methods of finding point correspondences. The former requires designing feature descriptors and is usually limited to keypoints that are detected by a detector, while the latter estimates dense pixel-level motion for consecutive frames instead of long-term motion. Recent work in particle video [8,25] predicts the motion of densely-sampled points based on feature correlation and pixel motion, exploits both sparse feature matching and optical flow, and achieves high accuracy in long-term pixel tracking.

Though dense point tracking has been studied in RGB images, its implementation in US is difficult. Most models for RGB images are trained on labeled datasets [6] or images generated from simulated 3D scenes [25]. However, it is difficult to simulate 2D US videos, because of the complexity of physical interaction between sound waves and tissue. Furthermore, US scans are operator-dependent. Labeling corresponding points is time-consuming and expensive, and requires training labelers to understand the particulars of US, such as artifacts.

To the best of our knowledge, this is the first report of enabling dense point tracking in US utilizing a particle video representation. Our novelty includes: (1) A new particle video model to track any number of points at the same time in US image sequences; (2) Lag-free tracking of points by utilizing self-supervised teacher-student learning: a teacher model that can view entire clips is used to train our model that estimates motion in a streaming manner.

## 2 Related Work

**Feature and Template-based Matching in US:** Feature matching has been used to track landmarks in US. Early methods used detectors and descriptors for RGB images such as FAST [23] and SIFT [14]. However, these methods do not consider the special structure and texture of US. Some methods use handcrafted features for US [2,4], but do not achieve real-time performance. Recent success of deep learning-based keypoint matching in RGB images raises interest in their applications to US, such as in Zhao *et al.* [24] and Shen *et al.* [19]. However, labels or external sensors are required for this supervised training.

Self-supervised or unsupervised learning has been investigated to reduce the effort of labeling. In [22], an autoencoder is trained to reconstruct patches and the latent space vector for each patch is used as features for tracking. Learning from data augmentation [21,13] and contrastive learning with teacher-student learning [12] have also been employed. However, these methods have been tested on a limited number of landmarks (usually on the CLUST dataset which has 1-5 annotated landmarks for each sequence [5]). Compared with these methods, our model can track an arbitrary number of points in one single forward pass.

**Optical Flow:** Optical flow estimates dense pixel-level motion and is similar to our work, but it is not widely applied in US. Classical optical flow methods

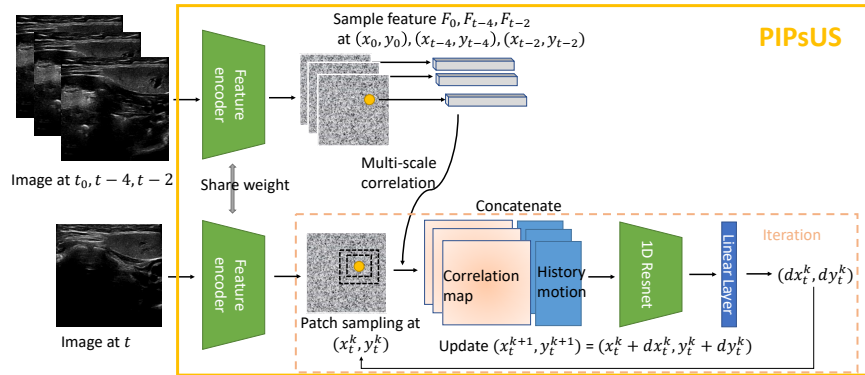


**Fig. 1.** PIPsUS architecture: PIPsUS enables streaming evaluation of point motion, estimating point motion at time  $t$  using motion and image feature history. The model encodes history and current images, and samples the feature of the tracked points on history feature maps. The correlation maps of the history feature and current feature maps are concatenated with the history motion. A 1D-Resnet encodes the information and a linear layer iteratively predicts the tracking update.

such as Lukas-Kanade [15], optimization-based flow [18], or in combination with block-matching [3] have been used for US, and deep learning optical flow such as LiteFlowNet [1], FlowNet [7] and PDD-Net [16] have also been investigated. However, these models only consider consecutive frames, making them more sensitive to drift and presenting artifacts. Unlike optical flow, our method uses both features and motion history to improve tracking performance.

**Track-any-point in RGB:** Our work is inspired by the problem of tracking-any-point (TAP), which estimates pixel correspondences in videos. Models such as PIPs [8], TAP-Net [6], and PIPs++ [25] have shown great potential, but they are trained with real labels or simulated scenes. By using established TAP models that ingress whole sequences, we developed a fine-tuning method to improve our model’s performance in US.

### 3 Methods

**PIPsUS Model.** We propose a model named Persistent Independent Particles in US (PIPsUS) to track points in US, as shown in Fig. 1. PIPsUS is inspired by PIPs++ [25], an improved model of Persistent Independent Particles (PIPs) [8], where pixel motions are modeled as moving particles in videos. It can track any pixels by investigating the entire video sequences instead of just consecutive frames as in optical flow. PIPs++ can operate on videos with various lengths while PIPs only inspects every 8 frames. However, PIPs++ inspects the entire video to predict point trajectories, so it can not predict in a streaming manner, and the computation and memory cost increases in long term.

PIPsUS first has a feature encoder that encodes the US images into feature maps. We use the same ResNet-based encoder as PIPs++ to enable the reuse of pre-trained weights to accelerate convergence. Features of the tracked points are sampled at prior frames by  $F_i = \text{bilinearsampling}(I_i, \mathbf{p}_i = (x_i, y_i))$ , where  $i \in \{0, t-4, t-2\}$ . Sampling from multiple frames allows the model to learn the original and current appearance of tracked points, while also keeping computation and memory cost constant. The same encoder is used on the new image  $I_t$  to generate a dense feature map. The new point location  $\mathbf{p}_t = (x_t, y_t)$  is estimated using an iterative method that showed great success in RAFT [20] and PIPs++. We assume zero-motion to start, so the initial location  $\mathbf{p}_t^0 = (x_t^0, y_t^0)$  is  $\mathbf{p}_{t-1}$ . For each iteration  $k$ , we sample an  $R \times R$  patch in the current frames’s feature map at  $\mathbf{p}_t^k$  as  $P^0, P^1, \dots, P^L$ , where  $L$  is the number of resolution layers. Feature  $F_i$  is correlated with these patches and the resulting correlation maps at each resolution are concatenated and reshaped into  $n L \times R^2$  vectors, where  $n$  is the number of points. Since the point motion should be consistent, we concatenate the most recent motion flow  $\mathbf{p}_t^k - \mathbf{p}_{t-1}^k, \mathbf{p}_t^k - \mathbf{p}_{t-2}^k, \mathbf{p}_t^k - \mathbf{p}_{t-3}^k$  and use a sinusoidal position embedding [8] to generate motion vectors which enables the model to utilize recent motion. A 1D-Resnet is used to further encode the concatenated motion and correlation vectors and to combine the feature correlation and recent motion, then a linear layer is used to predict the update  $\Delta \mathbf{p}_t^k$ . We update  $\mathbf{p}_t^{k+1} = \mathbf{p}_t^k + \Delta \mathbf{p}_t^k$  for the next iteration. At the beginning of the video, we pad the video with  $I_0$  and  $\mathbf{p}_0$  since our model needs image and location history.

**Self-supervised Teacher-Student Training:** To train the model without ground truth labels, we use two different pseudo-ground truth labels:

(1) PIPs++ teacher labels: We use point trajectories predicted by PIPs++ as labels to guide PIPsUS to predict the point motions. We use a weighted Huber loss because it is more robust against outliers than an L1 loss, preventing the model from overfitting possible wrong predictions in PIPs++:

$$L_t = \mu_t \sum_{k=0}^K w_k \text{HuberLoss}(\mathbf{p}_t^{gt}, \mathbf{p}_t^k) \quad (1)$$

$w_k$  is an increased weight with update iteration  $w_k = \gamma_{Iter}^{K-k-1}$  to encourage the model to learn the update function. The weight  $\mu_t = \gamma_{Time}^{T-t-1}$  increases with time to encourage the model to reduce drifting. We set  $\gamma_{Iter} = 0.8$  and  $\gamma_{Time} = 0.95$ .

(2) Simulation labels: We randomly transform ultrasound images with translation, intensity modulation, and noise addition to generate US videos with known motions. The loss is similar to Eq. 1 but with  $\gamma_{Time} = 1$ , and we choose L1 loss since the motion under our transformations is known.

We use the simulation to warm up the model. The model is then trained with PIPs++ labels plus 50% of the simulated labels, and we validate its performance on PIPs++ labels. We implement a zero-flow regularization with zero-motion videos to regularize model prediction. To let the model learn to correct its wrong predictions, the previous motion has a 70% chance of being the accurate flow with added Gaussian noise and 30% to be the model’s previous prediction. The points used for training are detected by the SIFT detector, with the contrast

**Table 1.** Number of collected videos and generated sequences in OUS dataset.

		Videos	Frames	# generated sequences	# keypoints per sequence
Pips++	Train	174	$65 \pm 42$	452	$18.75 \pm 14.33$
	Valid	57	$112 \pm 70$	278	$14.50 \pm 11.20$
	Test	45	$116 \pm 82$	225	$8.88 \pm 8.19$
Sim	Train	212	41	199	$20.53 \pm 13.78$
	Test	59	41	49	$13.00 \pm 9.57$

threshold set to 0.08 and the edge threshold set to 4. However, our model is not limited to SIFT in training and inference, and it can track any points.

## 4 Experiments

**Data:** (1) Neck and oral US (OUS): This is a private dataset containing 2D US sequences collected from 19 patients who underwent transoral robotic surgery, from January 2022 to October 2023 at the Vancouver General Hospital (Vancouver, BC, Canada). This study received ethics approval from the UBC Clinical Research Ethics Board (H19-04025). A BK3500 and a 14L3 linear 2D transducer (BK Medical, Burlington, MA) were used in the operation room for US imaging and a Polaris Spectra (Northern Digital, ON, Canada) was used to track the US transducer. PLUS [10] was used to record the US videos. The image depth is 4 cm at 9 MHz, with a frame rate of  $5.76 \pm 0.89$  fps. For each patient, the US scan included the neck, oropharynx, and the base of tongue (BOT) on the cancerous side, before and after the tongue retraction. Data from 12 patients are used for training, 4 patients for validation, and 3 patients for testing. We did not include the BOT scan for PIPs++ ground truth, since it mainly contains out-of-plane motions along the neck, but we kept the BOT images in the simulated sequences. For the PIPs++ labels, we split the recorded sequences into 20 frame-long sequences. For the simulated labels, we used the first frame in the videos to generate 41 frame-long sequences. The sequences that do not contain SIFT keypoints were discarded. Images were resized to  $256 \times 256$ . The final amount of data is summarized in Table 1.

(2) EchoNet [17]: EchoNet is a public dataset containing 2D videos of US cardio motion, shared under the Stanford University Dataset Research Use Agreement. We randomly select 200 videos for training, 50 videos for validation, and 50 videos for testing. Images were resized to  $256 \times 256$ . We use the same method to generate US sequences. The final amount of data used is included in Table 2.

**Training Details:** We train PIPsUS on the training splits of both datasets concatenated together. This results in a single model that we use for testing on each respective test split. The models were trained on an NVIDIA Tesla V100 and implemented in python 3.8, PyTorch-2.1.0, and CUDA-11.8. The weight of the encoder was initialized with the public weight of PIPs++. AdamW optimizer was used with a learning rate of  $5e-4$  for warmup, and  $1e-4$  for self-supervised teacher-student tuning. We warmed up the model with 10 epochs and then the

**Table 2.** Number of videos and generated sequences used in EchoNet dataset.

		Videos	Frames	# generated sequences	# keypoints per sequence
Pips++	Train	200	173 ± 46	1620	69.88 ± 19.97
	Valid	50	168 ± 38	392	68.65 ± 17.58
	Test	50	175 ± 47	410	75.87 ± 21.33
Sim	Train	200	41	200	75.36 ± 20.41
	Test	50	41	50	81.72 ± 24.36

**Table 3.** Quantitative evaluation on OUS. The L2 error is in pixels. \*\* The average time for PIPs++ to run inference on each sequence (20 frames) is 0.08 seconds.

Method	Simulation		Real Data		
	L2	NCC	L2	NCC	FPS
Fast NCC	6.65±6.25	0.83±0.19	22.84±27.91	0.82±0.19	145.2
RAFT	21.49±21.20	0.80±0.21	14.65±14.57	0.80±0.21	60.2
PIPs++	<b>0.94±0.72</b>	<b>0.95±0.10</b>	N/A	N/A	N/A**
PIPsUScorr	1.28±1.19	0.94±0.12	12.10±16.95	<b>0.84±0.19</b>	43.3
PIPsUS	1.10±0.88	<b>0.95±0.11</b>	<b>9.04±11.79</b>	<b>0.84±0.19</b>	34.6

model was trained with our self-supervised learning method for 50 epochs. The models with the lowest loss on the validation set were selected. The image batch size was 1 because the number of keypoints per batch varies.

## 5 Results

We compare our models with fast normalized cross-correlation (NCC) template matching [11], RAFT [20], PIPs++, and conduct an ablation study of our model with (PIPsUS) and without flow history (PIPsUScorr). RAFT was fine-tuned with US using L1-loss on optical flow warping for 5 epochs. We choose RAFT because it outperforms LiteFlowNet and FlowNet [20] and PDD-Net [16] is originally designed for 3D registration. We evaluated the performance on (1) simulated US sequences with smooth random affine motions and intensity changes and (2) real US sequences. Due to the lack of labeled ground truth on real US, we use the prediction from the teacher model PIPs++ as the ground truth, similar

**Table 4.** Quantitative evaluation on EchoNet. The L2 error is in pixels. \*\* The average time for PIPs++ to run inference on each sequence (20 frames) is 0.13 seconds.

Method	Simulation		Real Data		
	L2	NCC	L2	NCC	FPS
Fast NCC	6.40±6.60	0.83±0.22	5.05±10.56	0.93±0.13	19.3
RAFT	12.27±11.25	0.80±0.24	4.32±3.60	0.86±0.20	70.0
PIPs++	<b>0.90±0.75</b>	<b>0.96±0.11</b>	N/A	N/A	N/A**
PIPsUScorr	1.26±1.21	0.95±0.12	<b>2.27±2.62</b>	<b>0.94±0.11</b>	39.0
PIPsUS	1.07±1.04	0.95±0.11	2.40±3.15	<b>0.94±0.11</b>	15.4

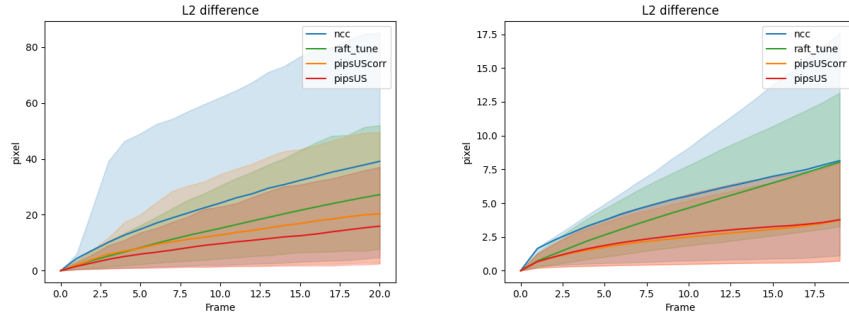


**Fig. 2.** L2 in different frames on real US sequence. Left: on OUS, right: on EchoNet. The line is average L2 and the shadow is 10 and 90 percentile.

to [9]. The quantitative evaluation includes L2 error and image-patch NCC, as shown in Table 3 for OUS and Table 4 for EchoNet. The L2 error evaluates the tracking accuracy, while the NCC quantifies the keypoint similarity.

In the simulation, PIPs++ has the highest accuracy and patch similarity, but PIPsUS is comparable to PIPs++ both on the OUS and EchoNet. PIPsUS and PIPsUScorr all demonstrate a large improvement in accuracy and similarity compared with fast-NCC and RAFT. In the real US, PIPsUS achieves the highest accuracy on OUS. PIPsUScorr performs the best on EchoNet, but PIPsUS is comparable. Again, PIPsUS and PIPsUScorr achieve higher accuracy in both datasets compared with Fast-NCC and RAFT. All methods perform better on EchoNet than OUS, and we expect this is because echocardiography contains smaller in-plane motions from standard views while freehand OUS contains larger motions and points can be out-of-plane. Thus, tracking points in EchoNet is easier. Fig. 2 shows the trend of L2 error; fast NCC and RAFT are both sensitive to drift. PIPs-like models view the features at different times, so their performance degrades more slowly. The results show the advantages of investigating multiple frames instead of just consecutive frames. The comparison between PIPsUS and PIPsUScorr shows that the motion history can improve motion estimation in OUS but not in EchoNet. We hypothesize that motion history can help generate a reasonable prediction when points have larger motion and are temporally out-of-plane, so its advantage is not shown in echocardiography where features remain in-plane. This is also shown in Fig. 3 which displays images of the tracked points and trajectories in OUS and EchoNet. More visualization is provided in the supplemental materials. We also evaluate the survival rate, which is the percentage of points that have an L2 error smaller than 50, as defined in PIPs++ [25]. In real EchoNet, the survival rate of the points at the end of sequences is 97.27% for fast NCC, and 100.00% for other methods. For OUS, the survival rate is 67.95% for fast NCC, 88.89% for RAFT, 90.27% for PIPsUScorr and 95.19% for PIPsUS, showing that PIPsUS is better at keeping track of points in OUS, which has more complicated motions.

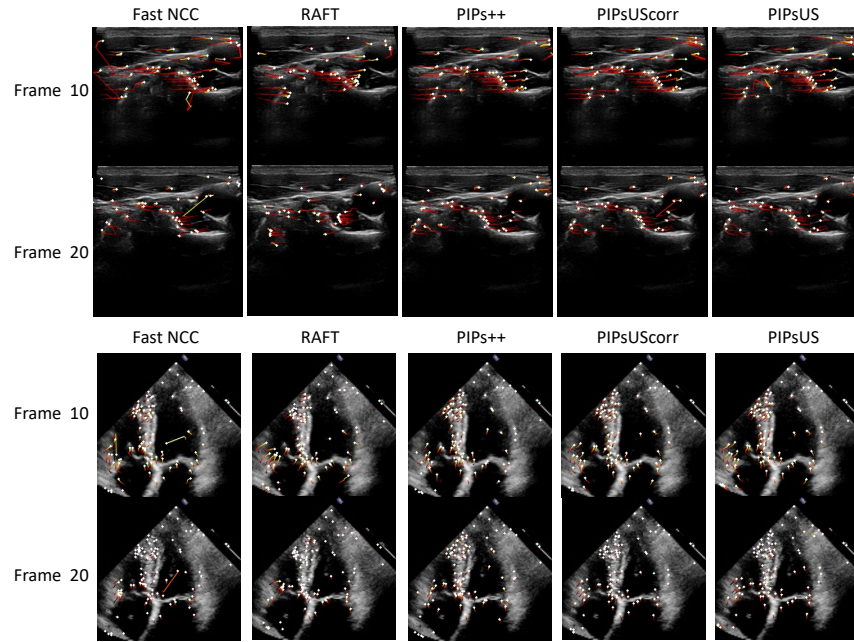


**Fig. 3.** Examples of tracked point trajectories in different frames on OUS (top 2 rows) and EchoNet (bottom 2 rows). The point is the current predicted keypoint locations and the colored line is the trajectory history. On OUS, in Frame 20 of PIPsUScorr and NCC, a point is correlated to a far away location. By using point motion history, PIPsUS avoids this.

**Limitations and Future Work:** Though we show improved short-term tracking, disappearing and reoccurring detection is required for long-term landmark tracking. We did not investigate other data augmentation methods, and US physics-based augmentation might improve the model’s robustness against deformation, shadows, and artifacts. Our model relies on feature correlation and temporal information without the awareness of point saliency. Integrating segmentation maps might allow the model to focus on tracking anatomically salient landmarks. These limitations have not been addressed in previous work for US, and we will investigate them for reliable long-term US point tracking.

## 6 Conclusions

We propose a lag-free new model utilizing particle video to track an arbitrary number of points utilizing dense feature maps and particles’ previous motion with constant memory cost, and can track points in real time. We develop a self-supervised teacher-student training strategy to train our model. Our model achieves higher accuracy compared with fast NCC and fine-tuned RAFT, and it is more robust to temporal drift.



## References

1. Al-Battal, A.F., Lerman, I.R., Nguyen, T.Q.: Object detection and tracking in ultrasound scans using an optical flow and semantic segmentation framework based on convolutional neural networks. In: ICASSP 2022-2022 IEEE International Conference on Acoustics, Speech and Signal Processing (ICASSP). pp. 1096–1100. IEEE (2022)
2. Alkhatib, M., Hafiane, A., Tahri, O., Vieyres, P., Delbos, A.: Adaptive median binary patterns for fully automatic nerves tracking in ultrasound images. *Computer methods and programs in biomedicine* **160**, 129–140 (2018)
3. Chuang, B.I., Hsu, J.H., Kuo, L.C., Jou, I.M., Su, F.C., Sun, Y.N.: Tendon-motion tracking in an ultrasound image sequence using optical-flow-based block matching. *Biomedical engineering online* **16**, 1–19 (2017)
4. Dall’Alba, D., Fiorini, P.: Bipco: ultrasound feature points based on phase congruency detector and binary pattern descriptor. *International journal of computer assisted radiology and surgery* **10**, 843–854 (2015)
5. De Luca, V., Banerjee, J., Hallack, A., Kondo, S., Makhinya, M., Nouri, D., Royer, L., Cifor, A., Dardenne, G., Goksel, O., et al.: Evaluation of 2d and 3d ultrasound tracking algorithms and impact on ultrasound-guided liver radiotherapy margins. *Medical physics* **45**(11), 4986–5003 (2018)
6. Doersch, C., Gupta, A., Markeeva, L., Recasens, A., Smaira, L., Aytar, Y., Carreira, J., Zisserman, A., Yang, Y.: Tap-vid: A benchmark for tracking any point in a video. *Advances in Neural Information Processing Systems* **35**, 13610–13626 (2022)
7. Evain, E., Faraz, K., Grenier, T., Garcia, D., De Craene, M., Bernard, O.: A pilot study on convolutional neural networks for motion estimation from ultrasound images. *IEEE transactions on ultrasonics, ferroelectrics, and frequency control* **67**(12), 2565–2573 (2020)
8. Harley, A.W., Fang, Z., Fragkiadaki, K.: Particle video revisited: Tracking through occlusions using point trajectories. In: *European Conference on Computer Vision*. pp. 59–75. Springer (2022)
9. Ihler, S., Kuhnke, F., Laves, M.H., Ortmaier, T.: Self-supervised domain adaptation for patient-specific, real-time tissue tracking. In: *Medical Image Computing and Computer Assisted Intervention—MICCAI 2020: 23rd International Conference, Lima, Peru, October 4–8, 2020, Proceedings, Part III* 23. pp. 54–64. Springer (2020)
10. Lasso, A., Heffter, T., Rankin, A., Pinter, C., Ungi, T., Fichtinger, G.: PLUS: Open-source toolkit for ultrasound-guided intervention systems. *IEEE Transactions on Biomedical Engineering* **61**, 2527–2537 (Oct 2014)
11. Lewis, J.: Fast normalized cross-correlation. *Industrial Light & Magic* **10**, 7 (2001)
12. Liang, H., Ning, G., Zhang, X., Liao, H.: Semi-supervised anatomy tracking with contrastive representation learning in ultrasound sequences. In: *2023 IEEE 20th International Symposium on Biomedical Imaging (ISBI)*. pp. 1–5. IEEE (2023)
13. Liu, F., Liu, D., Tian, J., Xie, X., Yang, X., Wang, K.: Cascaded one-shot deformable convolutional neural networks: Developing a deep learning model for respiratory motion estimation in ultrasound sequences. *Medical image analysis* **65**, 101793 (2020)
14. Machado, I., Toews, M., Luo, J., Unadkat, P., Essayed, W., George, E., Teodoro, P., Carvalho, H., Martins, J., Golland, P., et al.: Non-rigid registration of 3d ultrasound for neurosurgery using automatic feature detection and matching. *International journal of computer assisted radiology and surgery* **13**, 1525–1538 (2018)

15. Makhinya, M., Goksel, O.: Motion tracking in 2d ultrasound using vessel models and robust optic-flow. *Proceedings of MICCAI CLUST* **20**, 20–27 (2015)
16. Nicke, T., Graf, L., Lauri, M., Mischkewitz, S., Frintrop, S., Heinrich, M.P.: Realtime optical flow estimation on vein and artery ultrasound sequences based on knowledge-distillation. In: *International Workshop on Biomedical Image Registration*. pp. 134–143. Springer (2022)
17. Ouyang, D., He, B., Ghorbani, A., Lungren, M.P., Ashley, E.A., Liang, D.H., Zou, J.Y.: Echonet-dynamic: a large new cardiac motion video data resource for medical machine learning. In: *NeurIPS ML4H Workshop: Vancouver, BC, Canada* (2019)
18. Ouzir, N., Basarab, A., Lairez, O., Tourneret, J.Y.: Robust optical flow estimation in cardiac ultrasound images using a sparse representation. *IEEE transactions on medical imaging* **38**(3), 741–752 (2018)
19. Shen, C., He, J., Huang, Y., Wu, J.: Discriminative correlation filter network for robust landmark tracking in ultrasound guided intervention. In: *Medical Image Computing and Computer Assisted Intervention–MICCAI 2019: 22nd International Conference, Shenzhen, China, October 13–17, 2019, Proceedings, Part V 22*. pp. 646–654. Springer (2019)
20. Teed, Z., Deng, J.: Raft: Recurrent all-pairs field transforms for optical flow. In: *Computer Vision–ECCV 2020: 16th European Conference, Glasgow, UK, August 23–28, 2020, Proceedings, Part II 16*. pp. 402–419. Springer (2020)
21. Wang, Y., Fu, T., Wang, Y., Xiao, D., Lin, Y., Fan, J., Song, H., Liu, F., Yang, J.: Multi3: multi-templates siamese network with multi-peaks detection and multi-features refinement for target tracking in ultrasound image sequences. *Physics in Medicine & Biology* **67**(19), 195007 (2022)
22. Wulff, D., Hagenah, J., Ernst, F.: Landmark tracking in 4d ultrasound using generalized representation learning. *International Journal of Computer Assisted Radiology and Surgery* **18**(3), 493–500 (2023)
23. Wulff, D., Kuhlemann, I., Ernst, F., Schweikard, A., Ipsen, S.: Robust motion tracking of deformable targets in the liver using binary feature libraries in 4d ultrasound. *Current Directions in Biomedical Engineering* **5**(1), 601–604 (2019)
24. Zhao, C., Droste, R., Drukker, L., Papageorghiou, A.T., Noble, J.A.: Uspoint: Self-supervised interest point detection and description for ultrasound-probe motion estimation during fine-adjustment standard fetal plane finding. In: *International Conference on Medical Image Computing and Computer-Assisted Intervention*. pp. 104–114. Springer (2022)
25. Zheng, Y., Harley, A.W., Shen, B., Wetzstein, G., Guibas, L.J.: Pointodyssey: A large-scale synthetic dataset for long-term point tracking. In: *Proceedings of the IEEE/CVF International Conference on Computer Vision*. pp. 19855–19865 (2023)